Author Manuscript

Accepted for publication in a peer-reviewed journal

NIST National Institute of Standards and Technology • U.S. Department of Commerce

Published in final edited form as:

Dent Mater. 2014 December ; 30(12): 1316–1324. doi:10.1016/j.dental.2014.09.006.

Simultaneous Measurement of Polymerization Stress and Curing Kinetics for Photo-polymerized Composites with High Filler Contents

Zhengzhi Wang[a], **Forrest A. Landis**[b], **Anthony A.M. Giuseppetti**[c], **Sheng Lin-Gibson**[a], and **Martin Y.M. Chiang**[a,*]

[a]Biosystems and Biomaterials Division, National Institute of Standards and Technology, Gaithersburg, MD 20899

[b]Department of Chemistry, Penn State University – York Campus, York, PA 17403

[c]American Dental Association Foundation, Dr. Anthony Volpe Research Center, National Institute of Standards and Technology, Gaithersburg, MD 20899

Abstract

Objectives—Photopolymerized composites are used in a broad range of applications with their performance largely directed by reaction kinetics and contraction accompanying polymerization. The present study was to demonstrate an instrument capable of simultaneously collecting multiple kinetics parameters for a wide range of photopolymerizable systems: degree of conversion (DC), reaction exotherm, and polymerization stress (PS).

Methods—Our system consisted of a cantilever beam-based instrument (tensometer) that has been optimized to capture a large range of stress generated by lightly-filled to highly-filled composites. The sample configuration allows the tensometer to be coupled to a fast near infrared (NIR) spectrometer collecting spectra in transmission mode.

Results—Using our instrument design, simultaneous measurements of PS and DC are performed, for the first time, on a commercial composite with ≈ 80 % (by mass) silica particle fillers. The *in situ* NIR spectrometer collects more than 10 spectra per second, allowing for thorough characterization of reaction kinetics. With increased instrument sensitivity coupled with the ability to collect real time reaction kinetics information, we show that the external constraint imposed by the cantilever beam during polymerization could affect the rate of cure and final degree of polymerization.

Significance—The present simultaneous measurement technique is expected to provide new insights into kinetics and property relationships for photopolymerized composites with high filler content such as dental restorative composites.

[*]To whom all correspondence should be addressed (martin.chiang@nist.gov).

Keywords

Polymerization shrinkage stress; Tensometer; Infrared spectroscopy; Degree of conversion; Dental composites

Introduction

Photopolymerized composites are widely used in applications ranging from electrical and optical materials, structural materials, coatings and adhesives, to various biomedical applications such as dental restoration. Photopolymerization exhibits several advantages over other polymerization techniques, including excellent spatial and temporal control, fast curing rates under ambient conditions, and solvent-free processing (non-toxic/green) [1]. As monomers polymerize to form covalent bonds during the curing process, the volume of the resulting polymers can contract by significant amount, *e.g.* as high as 12 % of the volume contraction for dental resins [2]. Increasing the size or molecular mass of monomers, incorporating a larger amount of fillers, and tuning the reaction kinetics are some of the strategies to mitigate the adverse effects of polymerization shrinkage [2]; however, no approaches have been shown to fully eliminate polymerization shrinkage [3]. Further, enormous polymerization stress (PS) can develop for materials that shrink by as little as 1 % owing to the high modulus of these materials and can reduce the overall material performance. For example, in polymeric dental composites, considerable PS can develop at the tooth-composite interface that may lead to debonding, further tooth decay at the interface, and/or cracking of the tooth [4]. In coatings and adhesives, stress generated may lead to surface cracking and debonding. One of the common features in photopolymerization processes is that gelation can take place very fast, *e.g.* less than a second under a high-intensity irradiation condition. Therefore, it is important to accurately follow the curing kinetics of such fast reactions for a better assessment of the performance of monomers, as well as understanding and controlling the curing process. The object of this study is to introduce new instrumentation that can continuously monitor the development of PS and curing kinetics in real-time for polymer composites with filler content as high as ≈ 80 % by mass during photo-cure processing.

Polymerization shrinkage and stress are dictated by complex interplay among several factors, including curing kinetics (normally characterized by the degree of conversion, DC), development of resin shrinkage and modulus associated with DC, sample dimensions, and external constraint [5, 6]. Although there is generally a correlation between DC and PS, for practical purposes, DC is rarely used as a parameter to reduce PS since DC also correlates with other important material properties, *e.g.* mechanical properties [7], wear resistance [8], and the amount of leachable components [9]. Several methods have been developed to characterize PS for photo-polymerized materials, including stress-strain-analyzers [10], universal testing machines (with an extensometer) with almost zero compliance [11], single cantilever devices with fixed compliance [12], and cantilever beam-based instruments (a tensometer) with adjustable compliance [13, 14]. To understand reaction kinetics and PS development, it is necessary to measure these properties simultaneously. It is known that slight changes in sample configuration, irradiation, or instrumental compliance can greatly

affect the properties of complex photo-polymerizable systems. Therefore, there is a strong desire to combine these measurements for the same sample. To this end, Hsu *et al.* have demonstrated that Fourier Transform (FT) mid-infrared (mid-IR) spectroscopy can be coupled with a miniature cantilever system to effectively measure PS and DC simultaneously for photo-curing coatings [15]. In their study, FT-IR was collected in reflection mode; therefore, only the immediate surfaces (top few microns) were measured [16]. Later, near-IR (NIR) spectroscopy was shown to be capable of measuring double bond conversions in bulk samples in transmission mode. NIR exhibits lower molar absorptivity compared with the fundamental bands in the mid-IR region and shows two distinct peaks (6165 cm^{-1} and 4743 cm^{-1}) for C=C bond [17]. Lu *et al.* showed that PS and DC for a limited range of composites could be determined simultaneously by combining NIR spectrometry with a tensometer [18]. In that study, the dynamic range of the materials was limited by the instrument design (rigid beam), which reduced the sensitivity and accuracy of the instrumentation [14]. This design also required a sample with diameter of ≈ 6 mm, which was too large for accurate collection of transmission NIR at high filler contents due to the absorption and attenuation of the IR signal intensity. Using this instrument design, Lu *et al.* were able to measure composites with up to 30 % by mass filler content [18-20]. Many practical applications use a significantly higher amount of fillers (as high as 80 % by mass [21]) to improve the mechanical, tribological, and thermal properties of the materials [22].

In this study, a tensometer constructed according to our design criteria [14] was coupled to a high-speed data acquisition NIR spectrometer to enable real-time simultaneous measurement of PS and DC for highly filled polymer composites. Since temperature rise during photo-polymerization is usually a critical parameter in determining the applicability of the material, and reaction exotherm is also associated with the curing kinetics, the evolution of exothermic temperature is measured in parallel. Due to the existence of a vast number of monomer systems, studies related to methacrylate-based composites were chosen here. A capacitive displacement sensor and data acquisition devices/programs were incorporated in our tensometer system to improve the resolution and acquisition speed of the curing kinetics. Our results indicate that the simultaneous measurement can be performed on a model highly-filled composite (≈80 % by mass) at a high acquisition rate in excess of 10 data points per second, which gives sufficient data to accurately evaluate curing kinetics from the inception of polymerization. This higher resolution instrument also provides additional insight of curing kinetics under different degrees of constraint (achieved by adjusting sample position along the cantilever-beam of the tensometer). The null hypothesis tested was that changing the degree of constraint would have no effect on the curing kinetics, reaction exotherm, and final degree of polymerization.

Materials and Experiments ◆

In this investigation, a commercial dental composite (TPH Spectra™, Dentsply-Caulk, Milford, DE) was used as the test material to demonstrate the capabilities of the newly

◆Certain commercial materials and equipment are identified in this manuscript in order to specify adequately the experimental and analysis procedures. In no case does such identification imply recommendation or endorsement by the National Institute of Standards and Technology (NIST) nor does it imply that they are necessarily the best available for the purpose.

developed system for evaluating the development of PS and DC. TPH is a blue-light activated, urethane modified Bis-GMA/TEGDMA (50:50 mass ratio) based composite, filled primarily with barium boron aluminum silicate glass particles at 78 % by mass (≈ 57 % by volume).

A cantilever beam-based instrument (tensometer) presented in our previous study [14] has been further improved (described below) and a dispersive NIR spectrometer has been coupled to the instrument as shown in Fig. 1a. Using this device, an uncured composite (or resin) specimen was bonded with two quartz rods, the lower rod was fixed and the upper rod attached to a cantilever beam. Upon photo-polymerization, the composite shrinkage stress induced a deflection in the calibrated cantilever beam, which was recorded by a displacement sensor at the free end of the beam. The PS was then calculated through the beam formula [14]:

$$\sigma = \frac{F}{A} = \frac{6\delta EI}{\pi r^2 a^2 (3l - a)} \quad (1)$$

where σ is the PS and F is the force exerted by the sample shrinkage (see schematic in Fig. 1c); A and r are the cross-sectional area and the radius of the sample, respectively; δ is the beam deflection at the free end; E and I (= $wh^3/12$) are the Young's modulus and the moment of inertia of the beam, respectievly; h and w are the height and width of the beam cross-section, respectively; l and a are the length of the beam and the distance between the sample position and the clamped edge of the beam, respectively.

Instead of using a linear variable differential transformer (LVDT) as previous studies [13, 14, 18], a capacitive displacement sensor with 20-nm resolution (Driver Model: CPL190, Probe Model: C18-13, Lion Precision, St. Paul, MN) was used to provide more sensitivity for detecting the onset of shrinkage development (pre-gel stage). The analog data detected by the sensor were collected using the LabView software program (National Instruments, Austin, TX) via a 24-bit DAQ device (USB-2404-10, Measurement Computing, Norton, MA). Additionally, two micro stages with center aperture (GO®, Edmund Optics, Barrington, NJ) were assembled onto the base stand in X-Y configuration with the bottom quartz rod passing through their apertures, such that the alignment of the top and bottom rods can be easily achieved.

The remote NIR data acquisition was realized by configuring two optical-fiber cables (1 mm diameter, Multimode Fiber Optics, Inc., Hackettstown, NJ) onto the sides of the sample, with one cable connected to the IR light source (LS-1, Ocean Optics, Inc., Dunedin, FL) and the other to the NIR spectrometer (NIRQuest512-2.2, Ocean Optics, Inc., Dunedin, FL; Fig. 1b for a close view of the sample mounting region). The NIRQuest is a dispersive infrared spectrometer with a built-in diffractive grating-based optical bench, a 512-element InGaAs linear-array detector, and a 16-bit USB A/D converter. Although the dispersive spectrometer possesses relatively lower resolution, lower signal-to-noise ratio, and narrower spectral range than the bench top FT-IR instruments used in previous studies [15-18], it can provide much higher data acquisition rate and is more portable than FT-IR. The latter involves the movement of the interferometer optics and also the overhead associated with the computer

processing of the Fourier transform of the raw data. The scan rate of the system used here is up to 1000 Hz (integration time from 1 ms to 120 s) over the spectral range of 900 nm to 2200 nm (4500 cm^{-1} to 11100 cm^{-1}).

Simultaneous measurement of PS and DC were carried out using the tensometer and the NIR spectrometer as described above. The diameter and height of the composite sample were 2.5 mm and 2 mm, respectively. A non-tacky polytetrafluoroethylene (PTFE) sleeve (inner diameter: 2.5 mm, wall thickness: 0.4 mm) with an injection hole and a smaller air-venting hole was used to encase the rods and composite sample. The curing lamp (QHL75™ curing light, Dentsply-Caulk, Milford, DE) was attached to the lower rod with an opaque flexible light guide (10 mm diameter). The intensity of the curing light, measured by a Cure Rite radiometer (model # 8000, EFOS Inc., Williamsville, NY), was (500 ± 10) mW/cm^2 at the upper end of the bottom rod where the sample was bonded and took ≈ 0.4 s to reach the maximum after switch on. The irradiation start and end times were controlled by the LabView program through a controllable power outlet, such that the data collection and the photo-activation could be synchronized. For our measurements, the curing lamp was switched on at 20 s after the start of data collection and off at 60 s (*i.e.*, 40 s irradiation). According to the material manufacturer, this amount of irradiation was more than enough to cure a 2 mm thick sample that adopted in this study. The PS was recorded at a rate of 10 data points per second. The average of the data collected during the first 20 s (prior to irradiation) is used as the zero baseline. The NIR spectra were collected continuously at an integration time of 85 ms, which was also synchronized with the PS collection process. This optimal integration time was determined based on a series of test runs, which showed spectra of sufficient resolution and minimized noise. For the calculation of DC, the absorption peak of the methacrylate functional group centered at 6165 cm^{-1} (C=C-H stretching, first overtone) was used. The area under this peak was determined by subtracting a linear baseline across the edges of the peak for each spectrum obtained. Small variations in the intensity of the baseline were compensated for since the peak area was always calculated relative to the baseline of each individual spectrum. The DC was calculated by taking the peak area of the sample prior to the start of irradiation ($Area_{monomer}$) and at each point during the polymerization process ($Area_{polymer}$) based on the following formula [17, 23]:

$$DC = \left(1 - \frac{Area_{polymer}}{Area_{monomer}}\right) \times 100\% \quad (2)$$

To compare the spectra obtained by the dispersive NIR (D-NIR) and those by FT-IR in terms of resolution and acquisition rate, the uncured resin disks were measured using both instruments (FT-IR used: Nexus 670, XT-KBr beam splitter and MCT/A detector, Nicolet Instrument, Madison, WI), respectively. The FT-IR spectra (4500-6500 cm^{-1}) were collected through a NIR fiber port (Smart Fiberport, Nicolet Instrument, Madison, WI) with a 2 scans per spectrum and 8-wavenumber resolution (the typical parameters for real-time monitoring used in the literature), and also a 64 scans and 8 wavenumber resolution. To explore the effect of external constraint on the curing process, simultaneous measurements were performed when the upper rod was fixed at two different cantilever beam positions representing the higher and lower end of beam length (*i.e.* 6 cm and 20 cm from the fixed

end of the cantilever-beam), such that the rigidity of the effective beam experienced a near 40-fold change.

Experiments were conducted under a yellow light environment to minimize premature photopolymerization and at room temperature. The temperature increase due to the exothermic polymerization was also monitored at 10 Hz with a K-type miniature thermocouple (0.5 mm diameter, Omega Engineering Inc., Stamford, CT) embedded into the very edge (to avoid affecting the sample integrity) of the sample through the injection hole of the PTFE sleeve. In doing so, only temperature of the sample periphery was measured. For each set of experiments, three replicates were conducted.

Results and Discussion

A comparison study was conducted to determine spectral resolution and acquisition rate. As shown in Fig. 2a, the D-NIR spectrometer had an integration time of 85 ms (Δt, the average time span for collecting one spectrum) when scanned between 4500-6500 cm^{-1}; while FT-IR spectrometer required Δt = 1.7 s for the 2 scans 8 wavenumber resolution and Δt = 28 s for the 64 scans 8 wavenumber resolution. As expected, a spectrum with a lower noise can be obtained by increasing the scan number, and the FT-IR indeed gave higher spectrum resolution than the D-NIR. On the other hand, D-NIR provided a much faster acquisition rate (*ca.* 20 times faster) compared with FT-IR for a similar resolution that was desirable for studying the rapid curing kinetics. Fig. 2b shows the dynamic spectra of the composite using the D-NIR at different times during the polymerization. A continuous decrease of the aliphatic C=C peak intensity in the first overtone region (6165 cm^{-1}) and the combination region (4743 cm^{-1}) was observed. Due to peak overlap in the vicinity of the 4743 cm^{-1} peak, the 6165 cm^{-1} peak was selected for the DC calculation.

As shown in Fig. 3a, both the DC and PS data were simultaneously collected during polymerization. Note that in this study, the quartz rods used for bonding with the specimen were used without any surface treatment, which is different from those PS measurement systems reported in the literature [12-14], where the substrates usually need to be silanized to achieve the substrate-specimen interfacial integrity. Since the samples used here are self-adhesive composites and the current system is much more compliant than those in the literature, the adhesion between the sample and pure rods was found high enough to keep the interfacial integrity during the PS measurement (no difference was observed for the measurement of PS development by using silanized and non-silanized rods). Using the current system, we were able to collect abundant information to monitor DC and PS development upon irradiation, particularly at the early stage of the polymerization (inset). These data were significantly more comprehensive compared to previous studies [15-20, 23]. The inset plot shows that the development of PS started ≈ 5 s, which occurred at a later time compared to the onset of the DC (< 2 s). This behavior has previously been reported for similar materials [18, 20, 24] and is believed that the onset of stress development occurs near the gel point. Additionally, we observed a small negative PS (sample expansion) within the first few seconds, which was most likely due to the thermal expansion caused by the irradiation.

The key advantage for simultaneous PS and DC measurement is that these properties can be correlated directly (Fig. 3b), thus providing higher measurement confidence and more in-depth understanding of the network formation process. For the material studied, no obvious stress buildup was observed until DC reached ≈ 20%. If this point (*i.e.* the point where stress started buildup) is taken as the gel point, the observed gelation conversion is in large disagreement with those reported in the literature, where the typical values are well below 10 % for the dimethacrylate-based systems [25, 26]. The obvious discrepancy can be explained by the special sample configuration used in our tensometer system. The 2.5 mm sample diameter and 2 mm sample height correspond to a C-factor (ratio of bonded area to unbonded area) of 0.625 in this study; whereas the typical C-factor for PS measurement reported in the literature is close to or greater than 2 [12-14]. The significantly lower C-factor of our sample facilitates extensive material flow from the unbonded surfaces (*i.e.* the side face encased by the PTFE sleeve) during the pre-gel and early post-gel stages (where the sample is still quite viscous), which largely relieves and delays the PS buildup. Therefore, the onset of PS development is not necessarily representative of the sample gel point; for the system with low C-factor such as the one in this study, using PS development to approximate gel point could be considerably misleading. Upon an increase in the PS, a significant degree of stress developed (Fig. 3b) due to increases in the sample elastic modulus during the vitrification stage (*i.e.* polymer network transforms from rubbery state to glass state) [27].

Free radical photo-polymerizations are generally exothermic reactions. The actual temperature rise during photo-polymerization is the result of both reaction exotherm and heat generated by light irradiation. Contribution from the later factor can be determined by applying a second irradiation that has the same irradiation conditions as the first one on the post-cured sample [28, 29]. Fig. 4a shows real-time temperature rises from the combined contribution, contribution of light irradiation only, and their differences corresponding to reaction exotherm. Note that the temperature rise due to the photo-curing lamp only increased with irradiation time and gradually decreased once the light had been turned off. Measurement of reaction exotherm depends on two assumptions: the polymerization reaction must be completed prior to the second irradiation; and similar thermal conductivities and diffusivities through the uncured paste and cured solid must exist [29]. The first assumption was validated by the fact that the irradiance condition for polymerization far exceeded the minimum requirement from the manufacturer's recommendation (300 mW/cm^2 for 20 s). Additionally, monitoring of DC as a function of time (Fig. 3a) plateaued after the first few minutes after irradiation, indicating that minimal post-polymerization was occurring after 10 min. The second assumption was validated by using a prepared composite with the same formulation as the model composite without a photo-initiator. The same irradiation protocol was applied on the prepared paste and the changes in temperature of the composite were monitored. The results (Fig. 4b) show the temperature increase of the uncured and cured composites due to the irradiation have a nearly identical profile. This indicates that, for the material components studied, distributions of the light absorption coefficient in the composite are little changed from monomer state to polymer state.

With the improved instrument resolution and sensitivity, we determined the effects of external constraint on the rate of polymerization/gelation. These effects are important because virtually all applications of photo-polymerization occur under some constraints. In application where constraints vary greatly (such as filling material in dental repair), it is necessary to better understand the effect of constraints to better design materials. Many studies have assumed that constraint has minimal or no effects on the curing process and kinetics [30, 31]. Studies have shown that highly constrained samples resulted in higher DCs [18], and they proposed that the external tensile constraint increased free volume which can increase the mobilities of monomers and polymers, thus promote the polymerization reactions. In this study, the degree of mechanical constraint can be easily adjusted by the rigidity of the beam, which can be controlled by changing the sample position along the cantilever-beam of the tensometer. Fig. 5a shows the triplicate results of the DC development measured at beam length of 6 cm and 20 cm, corresponding to higher and lower constraints, respectively. Based on these real-time DC plots, the rate of polymerization (R_p) as a function of time (t) was obtained from the first derivative of the real-time DC curves by applying Hill's 4-parameter non-linear regressions on the raw DC data [32]; $R^2 > 0.995$ for all the regressions (Fig. 5b, data values given in Table 1). Clearly, DC developed faster and reached a slightly higher value for samples under the lower constraint. The maximum reaction rate (R_p^{max}) and the time it took to reach the maximum (t_r) were 7.4 ± 0.1 % s^{-1} and 1.7 ± 0.3 s for lower constrained samples and 4.9 ± 0.1 % s^{-1} and 3.2 ± 0.3 s for higher constrained samples. Additionally, DC after 30 min were 55.0 ± 1.2 % and 52.5 ± 1.8 % for lower and higher constrained sample, respectively. The relatively slower reaction rate under higher constraint is clearly evident in Fig. 5c, which plots the development of PS as a function of DC for the two constraint conditions. In addition, repeated measurements showed that peak reaction exotherm (ΔT_e^{max}) and the time it took to reach ΔT_e^{max} (t_e) were higher for the lower-constraint polymerization. ΔT_e^{max} was 8.0 ± 0.3 °C and 6.1 ± 0.3 °C, and t_e was 4.7 ± 0.3 s and 6.8 ± 0.1 s for lower and higher constrained samples, respectively (Fig. 5d). These results are consistent with DC data, *i.e.*, a lower reaction exotherm corresponds to a slower reaction rate.

Taken together, our results indicate external constraint indeed affected the curing kinetics and consequently, the reaction exotherm; thus, the null hypothesis tested was rejected. However, we note that our observation differs from previously reported trend obtained using other tensometer/FT-IR instruments by Lu *et al.* [18], in which the increased tensile constraint was found to be correlated with an increase in the final DC. In their study, lower sensitivity of the instrument and slower acquisition rate of the FT-IR did not provide sufficient information at the early stage of polymerization. Nevertheless, our trend agrees qualitatively with related studies involving the rate of reaction under confinement/constraint; for example, a recent study reported a decrease in the rate of reaction when the polymerization was confined inside a core-shell nanofiber [33]. The authors attributed this decrease to the obstruction of the cluster growth caused by steric restrictions, and the separation of the reacting area due to the formed clusters. Some early studies [34, 35] demonstrated a compressive stress would lead to an increase in the rate of reaction in solid-state polymerizations, since it would tend to reduce the strain energy at the monomer-polymer interface. Also, a recent study on polymerization under high pressure indicated

compression stress (pressure) decreased the intermolecular distance and the free volume of the monomer/polymer system and caused more cross-linked network than those polymerized under low pressure [36]. Based on these arguments, a possible explanation for the results observed in this study can be made. In our case, increasing the beam constraint tends to increase both the strain energy (potential) at the monomer-polymer interface and the free volume of the system during polymerization shrinkage of the sample. The former (*i.e.* increased strain energy) could be a direct reason for the observed slower reaction rate under higher constraint during the early stage of polymerization since the reaction is typically chemically-controlled dominated [37] (*i.e.* polymer chain propagates through the addition of the closest monomer unit without diffusion movement). After gelation, as the network becomes more cross-linked and restricted, polymerization reaction gradually becomes diffusion-controlled, in which the system's mobilities (largely related to the amount of free volume) play significant roles in determining the rate of reaction [38]. As a result, slightly higher reaction rates were observed for the higher-constrained sample (with more free volume) at the later stage of polymerization (*i.e.* after 5 s in Fig. 5b) and consequently, the final DC does not differ much for the two different constraint conditions. Further work is needed to elucidate this constraint-dependent polymerization process.

Conclusion

A cantilever-beam based instrument, incorporated with an in-situ, high-speed NIR spectrometer, has been developed to continuously monitor the polymerization stress, exotherm, and curing kinetics in real time for polymeric composites with high filler content. This development enables us to accurately follow the kinetics of fast photopolymerization and to unravel the complex interrelationship among curing kinetics, rate of reaction, and the polymerization stress, such that a better understanding and control of the curing process can be achieved. Our results indicate that the external tensile constraint slows down the curing process and restricts the extent of polymerization. Thus, correlation in the data collected under different constraints must be done with caution. The proposed experimental setups will facilitate further systematic examinations to find adequate mechanisms for the dependency of curing kinetics on the degree of constraint during the polymerization process.

Acknowledgements

This study is based on research that was funded partially by Interagency Agreement between the National Institute of Dental and Craniofacial Research and the National Institute of Standards and Technology, NIH/NIDCR [Y1-DE-7005-01]. Z. W. thanks Dr. Swarnavo Sarkar for his helpful discussion during the revision of the manuscript.

References

1. Nguyen KT, West JL. Photopolymerizable hydrogels for tissue engineering applications. Biomaterials. 2002; 23:4307–14. [PubMed: 12219820]
2. Dewaele M, Truffier-Boutry D, Devaux J, Leloup G. Volume contraction in photocured dental resins: the shrinkage-conversion relationship revisited. Dent Mater. 2006; 22:359–65. [PubMed: 16143380]
2. Chen CY, Huang CK, Lin SP, Han JL, Hsieh KH, Lin CP. Low-shrinkage visible-light curable urethane-modified epoxy acrylate/SiO2 composites as dental restorative materials. Compos Sci Technol. 2008; 68:2811–17.

3. Wen M, Scriven LE, McCormick AV. Differential scanning calorimetry and cantilever deflection studies of polymerization kinetics and stress in ultraviolet curing of multifunctional (meth)acrylate coatings. Macromolecules. 2002; 35:112–20.
4. Condon JR, Ferracane JL. Polymerization contraction stress of commercial composites. J Dent Res. 1998; 77:639.
5. Cramer NB, Stansbury JW, Bowman CN. Recent advances and developments in composite dental restorative materials. J Dent Res. 2011; 90:402–16. [PubMed: 20924063]
6. Watts DC, Satterthwaite JD. Axial shrinkage-stress depends upon both C-factor and composite mass. Dent Mater. 2008; 24:1–8. [PubMed: 17920115]
7. Li J, Li H, Fok ASL, Watts DC. Multiple correlations of material parameters of light-cured dental composites. Dent Mater. 2009; 25:829–36. [PubMed: 19395077]
8. Turssi CP, Ferracane JL, Vogel K. Filler features and their effects on wear and degree of conversion of particulate dental resin composites. Biomaterials. 2005; 26:4932–7. [PubMed: 15769527]
9. Ferracane JL. Elution of leachable components from composites. J Oral Rehabil. 1994; 21:441–52. [PubMed: 7965355]
10. Lee SH, Chang J, Ferracane JL, Lee IB. Influence of instrument compliance and specimen thickness on the polymerization shrinkage stress measurement of light-cured composites. Dent Mater. 2007; 23:1093–110. [PubMed: 17112580]
11. Condon JR, Ferracane JL. Reduced polymerization stress through non-bonded nanofiller particles. Biomaterials. 2002; 23:3807–15. [PubMed: 12164184]
12. Watts DC, Marouf AS, Al-Hindi AM. Photo-polymerization shrinkage-stress kinetics in resin-composites: methods development. Dent Mater. 2003; 19:1–11. [PubMed: 12498890]
13. Lu H, Stansbury JW, Dickens SH, Eichmiller FC, Bowman CN. Probing the origins and control of shrinkage stress in dental resin-composites: I. Shrinkage stress characterization technique. J Mater Sci Mater Med. 2004; 15:1097–103. [PubMed: 15516870]
14. Chiang MYM, Giuseppetti AAM, Qian J, Dunkers JP, Antonucci JM, Schumacher GE, Lin-Gibson S. Analysis of a cantilever-beam based instrument for evaluating the development of polymerization stresses. Dent Mater. 2011; 27:899–905. [PubMed: 21714998]
15. Stolov AA, Xie T, Penelle J, Hsu SL. Simultaneous measurement of polymerization kinetics and stress development in radiation-cured coatings: A new experimental approach and relationship between the degree of conversion and stress. Macromolecules. 2000; 33:6970–6.
16. Venhoven BAM, de Gee AJ, Davidson CL. Light initiation of dental resins: dynamics of the polymerization. Biomaterials. 1996; 17:2313–8. [PubMed: 8982470]
17. Stansbury JW, Dickens SH. Determination of double bond conversion in dental resins by near infrared spectroscopy. Dent Mater. 2001; 17:71–9. [PubMed: 11124416]
18. Lu H, Stansbury JW, Dickens SH, Eichmiller FC, Bowman CN. Probing the origins and control of shrinkage stress in dental resin composites. II. Novel method of simultaneous measurement of polymerization shrinkage stress and conversion. J Biomed Mater Res B. 2004; 71:206–13.
19. Lu H, Stansbury JW, Bowman CN. Impact of curing protocol on conversion and shrinkage stress. J Dent Res. 2005; 84:822–6. [PubMed: 16109991]
20. Stansbury JW, Trujillo-Lemon M, Lu H, Ding XZ, Lin Y, Ge JH. Conversion-dependent shrinkage stress and strain in dental resins and composites. Dent Mater. 2005; 21:56–67. [PubMed: 15681003]
21. Kleverlaan CJ, Feilzer AJ. Polymerization shrinkage and contraction stress of dental resin composites. Dent Mater. 2005; 21:1150–7. [PubMed: 16040118]
22. Lee LJ, Zeng CC, Cao X, Han XM, Shen J, Xu GJ. Polymer nanocomposites foams. Compos Sci Technol. 2005; 65:2344–63.
23. Yamasaki LC, De Vito Moraes AG, Barros M, Lewis S, Francci C, Stansbury JW, Pfeifer CS. Polymerization development of “low-shrink” resin composites: Reaction kinetics, polymerization stress and quality of network. Dent Mater. 2013; 29:169–79.
24. Braga RR, Ferracane JL. Contraction stress related to degree of conversion and reaction kinetics. J Dent Res. 2002; 81:114–8. [PubMed: 11827255]

25. Macosko CW, Miller DR. A new derivation of average molecular-weights of nonlinear polymers. Macromolecules. 1976; 9:199–206. [PubMed: 1263575]
26. Pfeifer CS, Wilson ND, Shelton ZR, Stansbury JW. Delayed gelation through chain-transfer reactions: mechanism for stress reduction in methacrylate networks. Polymer. 2011; 52:3295–303. [PubMed: 21799544]
27. Sakaguchi RL, Shah NC, Lim BS, Ferracane JL, Borgersen SE. Dynamic mechanical analysis of storage modulus development in light-activated polymer matrix composites. Dent Mater. 2002; 18:197–202. [PubMed: 11823010]
28. Alnazzawi A, Watts DC. Simultaneous determination of polymerization shrinkage, exotherm and thermal expansion coefficient for dental resin-composites. Dent Mater. 2012; 28:1240–9. [PubMed: 23018083]
29. Lloyd CH, Joshi A, McGlynn E. Temperature rises produced by light sources and composites during curing. Dent Mater. 1986; 2:170–4. [PubMed: 3462063]
30. Feilzer AJ, De Gee AJ, Davidson CL. Quantitative determination of stress reduction by flow in composite restorations. Dent Mater. 1990; 6:167–71. [PubMed: 2086289]
31. Min SH, Ferracane J, Lee IB. Effect of shrinkage strain, modulus, and instrument compliance on polymerization shrinkage stress of light-cured composites during the initial curing stage. Dent Mater. 2010; 26:1024–33. [PubMed: 20684977]
32. Moraes RR, Garcia JW, Barros MD, Lewis SH, Pfeifer CS, Liu JC, Stansbury JW. Control of polymerization shrinkage and stress in nanogel-modified monomer and composite materials. Dent Mater. 2011; 27:509–19. [PubMed: 21388669]
33. Reddy CS, Arinstein A, Zussman E. Polymerization kinetics under confinement. Polym Chem. 2011; 2:835–9.
34. Bamford CH, Eastmond GC, Ward JC. Effect of mechanical stress on some solid-state polymerizations. Nature. 1961; 192:1036–8.
35. Adler G, Ballantine D, Baysal B. The mechanism of free radical polymerization in the solid state. J Polym Sci. 1960; 48:195–206.
36. Béhin P, Stoclet G, Ruse ND, Sadoun M. Dynamic mechanical analysis of high pressure polymerized urethane dimethacrylate. Dent Mater. 2014; 30:728–34. [PubMed: 24802521]
37. Lovell LG, Stansbury JW, Syrpes DC, Bowman CN. Effects of composition and reactivity on the reaction kinetics of dimethacrylate/dimethacrylate copolymerizations. Macromolecules. 1999; 32:3913–21.
38. Sideridou I, Tserki V, Papanastasiou G. Effect of chemical structure on degree of conversion in light-cured dimethacrylate-based dental resins. Biomaterials. 2002; 23:1819–29. [PubMed: 11950052]

Highlights

We develop new system for real-time measuring shrinkage stress and curing kinetics.

The system shows unprecedented combination of sensitivity and resolution.

Simultaneous measurement can be performed on composites with high filler content.

Measurement of reaction exotherm during polymerization is justified.

Mechanical constraint could affect polymerization kinetics.

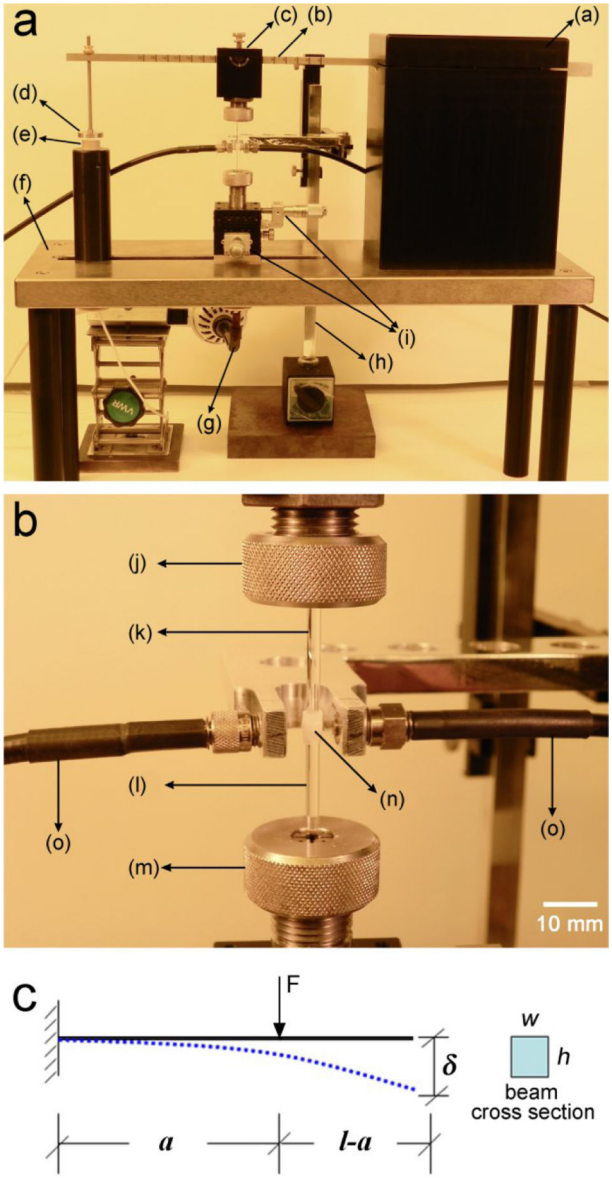

Fig. 1.

Photographs of the tensometer for the simultaneous measurement of polymerization stress and degree of conversion from a) overall view, and b) close view of the sample mounting region (data acquisition devices and spectrometer not shown): (a) cantilever-beam holder; (b) cantilever beam (stainless steel, 6.36 mm width, 6.35 mm height, 24.5 cm length with effective beam length ranging from 6 cm to 20 cm); (c) upper collet holder; (d) flat metal target; (e) probe of the sensor; (f) base stand; (g) curing light guide; (h) NIR cable holder; (i) X-Y stages; (j) upper collet; (k) upper quartz rod; (l) lower quartz rod; (m) lower collet; (n) sample encased by polytetrafluoroethylene sleeve; (o) NIR optical fibers. c) schematic of cantilever beam configuration for polymerization stress measurement.

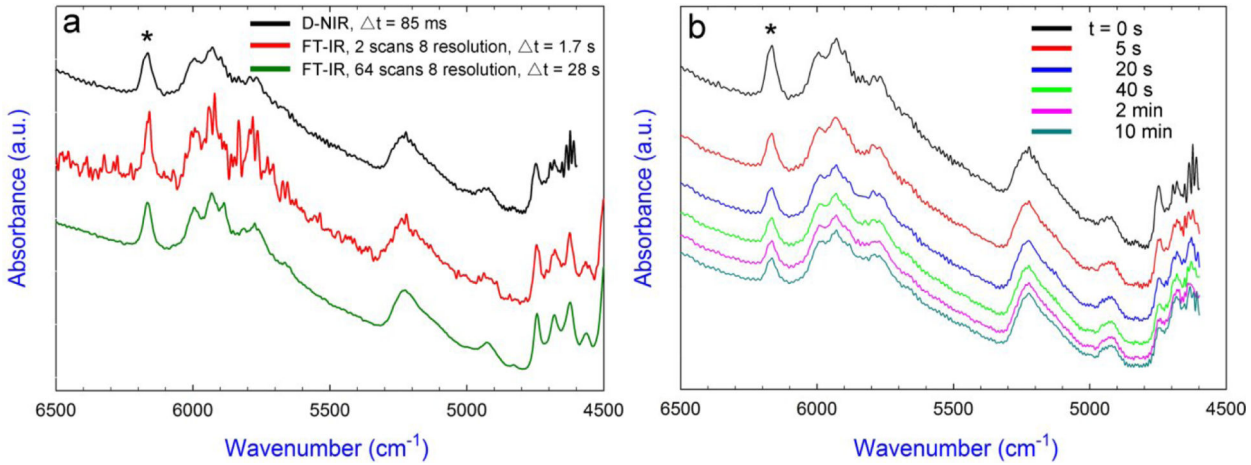

Fig. 2.

a) The absorption spectra of uncured TPH collected using the D-NIR and FT-IR instruments with two different coadded scan numbers (Δt, the average time span for collecting one spectrum). The level of noise in the D-NIR spectrum was reduced relative to that in the FT-IR spectrum using 2 scans and 8 resolution. b) The absorption spectrum of TPH during polymerization collected by real-time D-NIR at various intervals (t, the real time after irradiation starts). Absorptions associated with the methacrylate $=CH_2$ bonds (first overtone) are highlighted by asterisks at 6165 cm^{-1}.

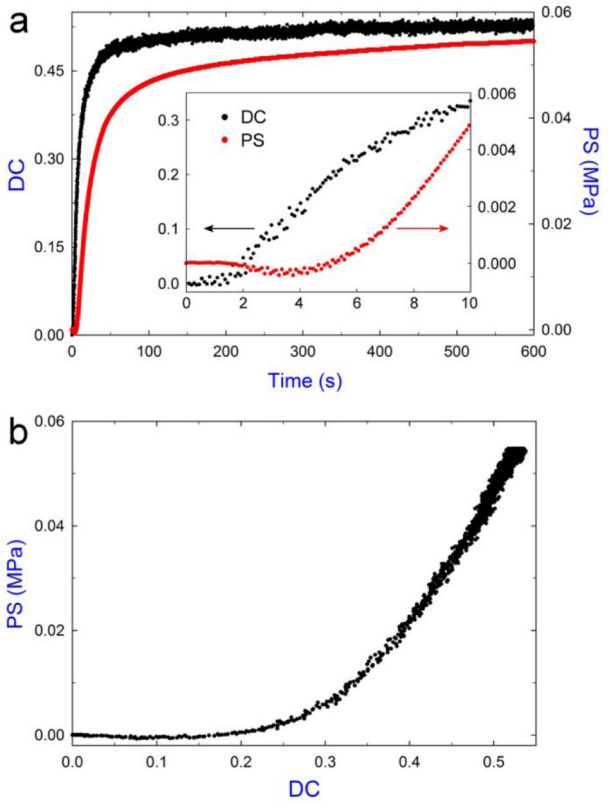

Fig. 3.

Typical results obtained from the simultaneous measurement test of a TPH sample. a) The development of polymerization stress (PS) and degree of conversion (DC) in the first 10 min after irradiation. The inset shows the data in the first 10 s. b) The PS development as a function of DC.

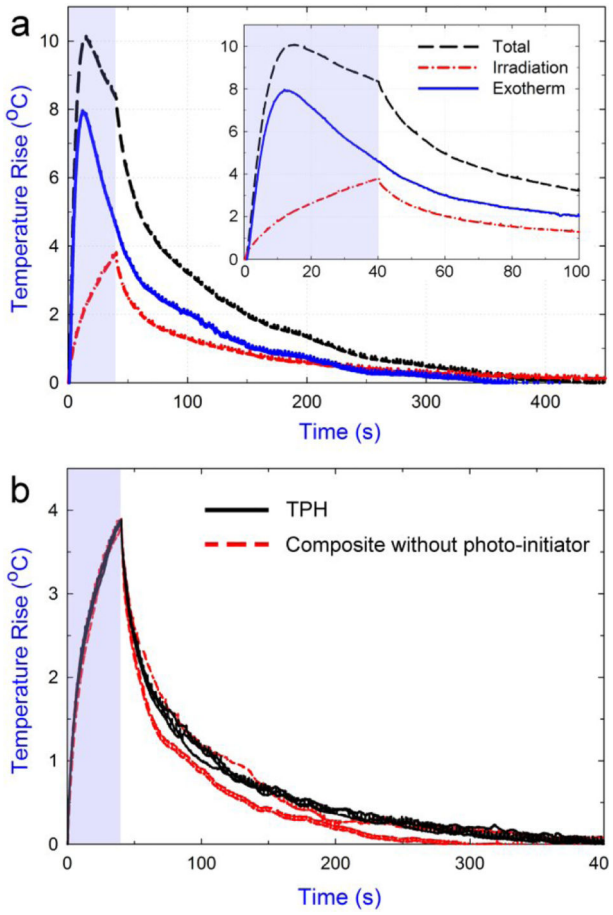

Fig. 4.

Typical results of the temperature measurement. a) Superposition of the temperature rise during 1st (Total) and 2nd (Irradiation) irradiation allows the calculation of reaction exotherm (inset shows the data in the first 100 s). b) Triplicate measurements of temperature rise for the cured TPH and the prepared composite paste without photo-initiator under the same irradiation conditions. Shaded regions indicate irradiation time.

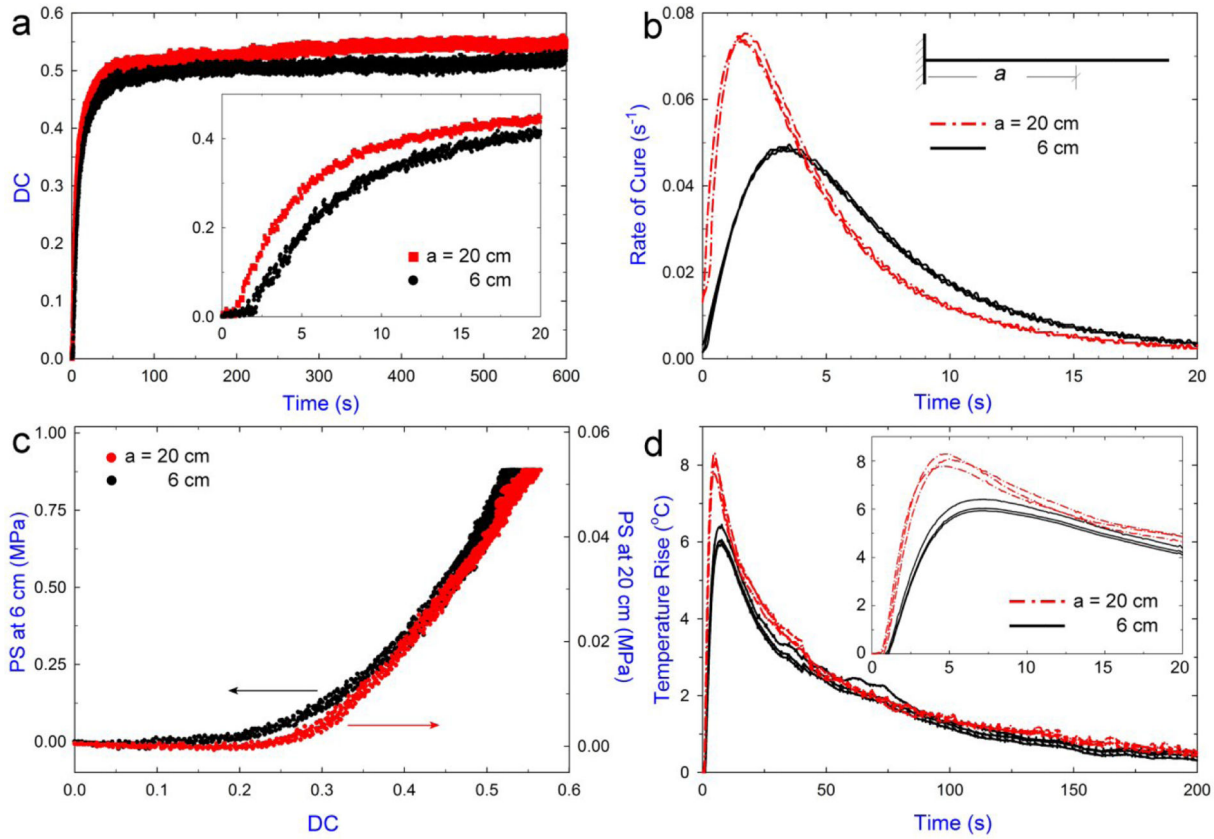

Fig. 5.

a) Comparison of the DC development measured at two sample positions in the simultaneous measurement tests of TPH composites; inset shows the data in the first 20 s. b) Reaction rate profiles at the two sample positions. c) The PS development as a function of DC at the two sample positions. d) The calculated reaction exotherm for the polymerization at the two sample positions; inset shows the results of the first 20 s.

Table 1

Mean values (n = 3) of the PS, DC, exothermic temperature rise, and related kinetic parameters induced at the two sample positions (mean value (standard deviation)). Both PS and DC values were taken at 30 min after irradiation.

		DC and kinetics			Reaction exotherm	
Sample position (cm)	**PS (MPa)**	**DC (%)**	**R_p^{max} (% s^{-1})**	**t_r (s)**	**ΔT_e^{max} (°C)**	**t_e (s)**
6	0.891 (0.013)	52.5 (1.8)	4.9 (0.1)	3.248 (0.256)	6.142 (0.254)	6.776 (0.101)
20	0.055 (0.001)	55.0 (1.2)	7.4 (0.1)	1.654 (0.282)	8.036 (0.259)	4.721 (0.338)